

Dynamic mechanical properties of murine brain tissue using micro-indentation

D. B. MacManus^a, B. Pierrat^a, J. G. Murphy^b, M. D. Gilchrist^{a*}

^a*School of Mechanical & Materials Engineering, University College Dublin, Dublin, Ireland*

^b*Department of Mechanical & Manufacturing Engineering, Dublin City University, Dublin, Ireland*

**Corresponding Author*

Tel: +353 1 716 1890, +353 1 716 1991

Email: david.mac-manus@ucdconnect.ie (D.B. MacManus), baptiste.pierrat@ucd.ie (B. Pierrat),
michael.gilchrist@ucd.ie (M. D. Gilchrist)*, jeremiah.murphy@dcu.ie (J. G. Murphy).

Abstract

Significant advances have been made in recent decades to determine the macro-scale properties of brain tissue in compression, tension, shear and indentation. There has also been significant work done at the nanoscale using the AFM method to characterise the properties of individual neurons. However, there has been little published work on the micro-scale properties of brain tissue using an appropriate indentation methodology to characterise regional differences at dynamic strain rates. This paper presents a novel micro-indentation device that has been developed and used to measure the dynamic mechanical properties of brain tissue. The device is capable of applying up to 30/s strain rates with a maximum indentation area of 1500 μm^2 . Indentation tests were carried out to determine the shear modulus of the cerebellum (3.59 ± 1.27 kPa) and cortex (7.05 ± 3.92 kPa) of murine brain tissue at 30/s up to 14% strain. Numerical simulations were carried out to verify the experimentally measured force-displacement results.

Keywords: Traumatic Brain Injury (TBI), Cortex, Cerebellum, Sneddon, Finite Element Analysis.

1. Introduction

The head is one of the most vulnerable parts of the human anatomy and injuries sustained to the head are often life-threatening or have severe consequences. The Centre for Disease Control and Prevention reports that every year 1.7 million people suffer from a traumatic brain injury (TBI) in the United States. Of the 1.7 million injuries, 52,000 die, 275,000 are hospitalized and 1.365 million are treated and released from an emergency department (Faul et al., 2010). Traumatic brain injuries (TBIs) are typically classified as being either focal or diffuse. Focal injuries occur over a localized area (contusion), whereas diffuse injuries occur globally throughout the organ (ischemia). Traumatic brain injury is caused by a mechanical force acting upon the head (Gaetz, 2004), resulting in linear and rotational accelerations that occur as a combination of compression, tension and shear (El Sayed et al., 2004; Rashid et al., 2012, 2013; Giordano, 2013). Rotational accelerations cause shearing of axons which can lead to traumatic axonal injury (TAI) and rupture of vasculature, while linear accelerations cause translational impacts of the brain against the skull, causing coup contusions and cavitation at the contrecoup site of injury (El Sayed et al., 2004). Indentation is a complex loading modality as it applies compression, tension and shear deformation fields to the material, however, it can be assumed to be purely compressive as tension only occurs at the edge of the contact region (Lin et al., 2009).

In recent years traumatic brain injury has received much public attention and has become a focus area for research with many laboratories creating 3D finite element models of the head and brain (Kleiven & von Holst, 2002, Mao et al., 2013, Horgan et al., 2003, Willinger et al., 1999). However, to construct an accurate head model, detailed anatomically correct geometry and accurate constitutive data of brain tissue are required to correctly predict the stresses and strains produced in the brain during injury scenarios. There are a number of precise anatomically correct head and brain models currently in use. However, many of them do not have access to accurate, region-specific constitutive data for neural tissue. A number of studies have been published on the macro-scale properties of brain tissue in compression, tension, shear and indentation (Jin et al., 2013, Pervin & Chen, 2009, Sanborn et al., 2011, Haslach et al., 2014, Cheng & Bilston, 2007). There has also been significant work conducted at the nanoscale using the AFM method to characterize the properties of individual neurons (Bernick et al., 2010, Mustata et al., 2009, Lu et al., 2006). However, to the best of the authors' knowledge, there has been little published work on the micro-scale properties of brain tissue using the micro-indentation method to characterize the differences between grey and white matter at dynamic strain rates. This difference between white and grey matter is due to the microstructure and neuroarchitecture of the tissues. White matter consists of long, bunched axons that connect different regions of the brain and can range in diameter from 1-20 μ m (Gaetz, 2004).

Grey matter contains the neuronal cell bodies, or soma, from which axons and dendrites extend, and is usually found in the upper cortical surface and in some deeper brain structures such as the basal ganglia (Rashid et al., 2012, Prange & Margulies, 2002, Hendelman, 2006). Current devices lack the resolution to obtain micro-scale tissue properties of white and grey matter. Therefore, to remedy this and add to the existing body of knowledge on brain tissue mechanical properties, the authors have designed a custom-built micro-indentation device to test these properties at the micro-scale. This paper presents the design and validation of the device which will be used to investigate the mechanical properties and regional differences of brain tissue at dynamic rates. The device described herein is capable of performing micro-indentation tests up to a maximum indentation depth of 3mm at velocities reaching 1000mm/s.

2. Materials & Method

2.1 Device Design

The custom-built micro-indentation device is outlined in Fig. 1 and uses a modular design to allow for easy construction, repair, and replacement of possible testing modules (compression/tension, shear, indentation). The device consists of three major components, the 3D-printed force-sensing probe stage, the linear stage (ZABER-LSQ), which moves the force-sensing probe stage in the vertical direction at speeds reaching 1m/s, and the load cell subsystem which can be adapted easily, depending on the type of test being conducted.

The linear stage (ZABER A-LSQ300D, Zaber Technologies Inc, British Columbia, Canada) is oriented vertically and has a 300mm travel range. The linear stage consists of a stepper motor that drives a lead screw which translates the stage along its axis. The stage is capable of reaching a maximum speed of 1000mm/s and a minimum speed of 0.001211mm/s. The maximum achievable acceleration and deceleration of the device is 100,000mm/s². The stage has a microstep size of 1.984μm and repeatability is <3μm. The peak and maximum continuous thrust are both 18N, and the maximum cantilever load is 800Ncm. The stepper motor is connected to the ZABER Motor Controller (A-MCB-2, Zaber Technologies Inc, British Columbia, Canada) that interfaces with a PC and can be controlled through the ZABER Console.

The force sensing component for indentation testing is the FemtoTools FTS-10000 Microforce Sensing probe (FemtoTools AG, ZH, Switzerland), which sits inside a protective 3D-printed casing. The probes are capable of measuring forces in the range of ±10,000μN with a 5000μN/V sensitivity and resolution of 0.5μN at 10 Hz. The standard probe geometry has a thickness of 50μm with a 50μm wide flat tip that tapers to 300μm width at an angle of 45°. The

overall length of the probe is 3mm. See Fig. 2 for more detailed dimensions. The probes connect to a FemtoTools FT-SC01 Force Acquisition System (FemtoTools AG, ZH, Switzerland) which interfaces with a PC, resulting in easy to use controls and displays the results directly on screen in μN against time. The Force Acquisition System is capable of having up to 4 probes connected at once. The system has 14-Bit data acquisition with a sensor readout bandwidth of 10kHz, and is powered via USB. The probes in their 3D printed protective housing are attached to the linear stage and the height of the specimen stage is adjusted according to the desired indentation depth in order to protect the probe from damage.

2.2 Theory

Indentation has been used previously to study the local mechanical properties of soft tissues (Elkin et al., 2011, Gefen & Margulies, 2004). The deformations produced during an indentation are often infinitesimal when compared with the overall length-scale of the specimen being tested. The contact stresses are highly concentrated close to the contact region and they decrease rapidly with increasing distance from the point of contact (Johnson, 1985). Therefore, it is convenient to approximate the region being indented as a semi-infinite half-space. The idealisation of bodies with arbitrary surface profile being regarded as semi-infinite and having a plane surface is made almost universally in elastic contact stress theory as it simplifies the boundary conditions and allows the use of the large body of elasticity theory, which has been developed previously for the elastic half-space (Johnson, 1985). These same assumptions were made by Sneddon when he formulated the relation between load and penetration for a punch of arbitrary profile (Sneddon, 1965). In his paper Sneddon presented a solution of the axisymmetric Boussinesq problem for which he derived simple formulae for the depth of penetration of the tip of a punch of arbitrary profile and for the total load which must be applied to the punch to achieve this penetration.

In this study we exploit Sneddon's work and adjust his equation for spherical tipped indenters according to Pharr et al. (2009), to obtain the modified Sneddon equation for square tipped indenters (Eqn. 1):

$$P = \frac{\beta A \mu a h}{1 - \nu} \quad (1)$$

$$\beta_{square} = 1.012$$

where a is the contact radius ($A = \pi a^2$), h is the indentation depth, ν is Poisson's ratio (assumed here to be 0.5), μ is the shear modulus, and β_{square} is the compensating factor for square tipped indenters, with $\beta = 1$ recovering Sneddon's solution. The modified Sneddon equation is used to determine the shear and Young's moduli of the brain tissue.

The strain was calculated using the widely accepted equation for calculating indentation strain (Lin et al., 2009) and adjusted accordingly to fit the square cross section geometry of the indenter tip used in this study in order to calculate the values for strain and strain-rate:

$$\varepsilon = \sqrt{\frac{h^2 \pi}{A}} \quad (2)$$

$$\dot{\varepsilon} = \frac{\varepsilon}{t}$$

where h is the indentation depth, and A is the contact area of the probe.

2.3 Experiment

A set of experiments were performed to validate the design. Eleven mice were collected following a recent cull in University College Dublin's Biomedical Facility. The brains were removed from the animals and tests were completed within 6h post-mortem in order to reduce the amount of protein decay and necrosis, since this has previously been shown to reduce the stiffness of the tissue (Fountoulakis et al., 2000, Isidre et al., 2007). A midline incision was made through the skin across the top of the head to gain access to the skull. A second midline incision, moving anteriorly from the occipital condyle, was made through the skull. Two lateral incisions were then made at an anterior and posterior point of the midline incision so that the bone could be removed and allow access to the brain. The brain was then separated from the spinal cord and removed from the skull. Indentation tests at a strain-rate of 30/s up to 14% strain were conducted at six locations on each brain. The indentation sites were located at the left and right anterior cortex, left and right posterior cortex, and left and right cerebellum, as indicated in Fig. 3.

Indentations were performed at room temperature (22°C), to a depth of 20µm (14% strain) at 30/s to characterize the properties of mouse brain at impact speeds. A total of 11 brains were tested with 6 tests conducted per brain. The results were post-processed in MATLAB using a moving average filter to remove any unwanted noise from the raw data and were then fitted to the modified Sneddon model (Eqn. 1) to determine the shear and Young's moduli.

2.4 Numerical Investigation

The data obtained from the experiment were applied to numerical models of the test setup recreated in FEBio 2.0 (Maas et al., 2012). Analyses were performed for the results obtained for both the cortex and cerebellum at 30/s strain rate. The indenter tip geometry was modeled following the

FemtoTools Force Sensing Probe dimensions (see Fig. 2). The indentation was modeled by creating an editable mesh, and applying a 20 μ m downwards displacement to the elements that lie below the square cross section of the indenter tip. It was assumed for small displacements that only the square cross-section of the probe would be in contact with the tissue. The material was modeled using the Ogden model (1972), Eqn. 3, with the material parameters given in Table 1. The experimental results behind these data are described in Section 3.1.

$$W = \frac{2\mu_0}{\alpha^2} (\lambda_1^\alpha + \lambda_2^\alpha + \lambda_3^\alpha - 3) \quad (3)$$

where W is the strain energy function, μ is the shear modulus, α is the stiffening parameter, and λ is the stretch ratio.

Table 1. Finite Element Model Material Parameters

Region	Density (kg/m ³)	Bulk Modulus (MPa)	C1 (=2 μ_0) (MPa)	C2-C6 (=2 μ_{1-5}) (MPa)	M1 (= α_1)	M2-M6 (= α_{2-6})
Cortex	1010	70.5	0.01410	0	1	1
Cerebellum	1010	35.9	0.00718	0	1	1

It is the authors intent to determine the initial (linear) parameters. Therefore, α was chosen to be 1 to approximate a linear response of the tissue. The geometry of the brain tissue consisted of a 3D cuboid with dimensions 6x3mm with an encastre boundary condition applied to the bottom face of the model to account for the adhesion of the brain to the specimen stage. The mesh consisted of biased hexahedral elements. Force-displacement data were then extracted from the results of the simulation and compared with the experimental results to verify material parameters obtained from the Sneddon model.

3. Results

3.1 Experiment

The experimental results from this custom-designed device show that cortex of the mouse brain is significantly stiffer than the cerebellum (statistical difference being $p < 0.01$), which is consistent with recent observations by Elkin et al. (2011). Indentations were performed to a depth of 20 μ m at 30/s, the average cerebellum peak force was recorded as 14.6 μ N and the peak force for cortex tissue was 32.1 μ N.

Student's two-sample T-test results showed no statistically significant difference for stiffness

between the left and right regions of the brain. Therefore, the average values for the cortex and cerebellum were taken by using the data for both left and right hemispheres for the three regions. The shear modulus for the cerebellum was found to be 3.59 ± 1.27 kPa at 30/s; the shear modulus for the cortex was 7.05 ± 3.92 kPa at 30/s. However, student's T-tests showed a significant difference between the cerebellum and cortex, with $p = 0.0015$. These results were used in the numerical models described earlier to determine their efficacy and are summarised in Table 2.

Table 2. Experimentally Determined Material Properties of Murine Brain

Region	Strain Rate (1/s)	%Strain	$\mu \pm SD$ (kPa)	$E \pm SD$	p-value
Cortex	30	14	7.05 ± 3.92	21.15 ± 11.76	0.0015
Cerebellum	30	14	3.59 ± 1.27	10.77 ± 3.81	

3.2 Numerical Investigation

Numerical simulations were performed for both the cortex and cerebellum to determine the efficacy of the results obtained from the analytical solution (Eqn. 1). The numerical predictions were fitted to the experimentally determined force-displacement curves to determine the accuracy of the analytically determined results. The mean reaction forces found numerically were $37.7 \mu\text{N}$ and $19.2 \mu\text{N}$ for the cortex and cerebellum, respectively. These results are $\sim 20\%$ higher than those determined experimentally, as indicated in Fig. 4. The R^2 values for fitting the numerical force-displacement curve to the experimental curve is 0.85 for cortex tissue and 0.76 for the cerebellum. It is the author's belief that this error results from assuming the contact area of the probe to be perfectly square, whereas due to the tapered sides on the actual probes, the contact area is possibly larger than the square area assumed in calculations. If the brain tissue deforms in such a way that allows for the tapered sides to come into contact with the tissue, this would increase the contact area and result in a lower modulus calculated by the analytical solution. However, the device is successfully able to determine the initial elastic properties of brain tissue.

4. Discussion

This paper presents the design and verification of a new device for conducting micro-indentation experiments on brain tissue at dynamic rates. As brain tissue is considered one of the softest and most difficult tissues to test, the device must be able to sense loads on the micro-Newton scale and perform indentations at strain rates which are experienced during surgical procedures, as well as those known to cause injury i.e. $>10\%$ strain and $>10/\text{s}$ (Rashid et al., 2012). The micro-indentation

device is capable of performing impacts up to a maximum velocity of 1000mm/s; depending on the geometry of the indenter, these can reach large strain rates >1000/s. The force-sensing acquisition module of the device records data from the probes at 10kHz with a 14-bit accuracy allowing for a maximum accurate measurement of up to 30/s strain rate with the current indenter tip geometry.

A set of numerical and experimental tests were designed in order to verify the new device. The results from the indentation experiments show that the cerebellum is significantly softer than the cortex, which is consistent with other results (Elkin et al., 2011). No other studies currently available in the literature appear to compare the mechanical properties of the cortex and cerebellum, or at strain rates larger than 10/s for micro-indentation. The results also showed no significant difference between the left and right hemispheres, which is in agreement with the results of Prevost et al. (2011). Therefore, the results presented here are a significant addition to the current scientific literature on the dynamic and regional mechanical properties of brain tissue. The numerical studies using FEBio 2.0 (Maas et al., 2012) were conducted using the properties obtained for brain tissue from experiment and were in reasonable agreement with the experiment, thereby validating the measured properties ($R^2 = 0.76$, and 0.85 for the cerebellum and cortex respectively). It is believed that higher R^2 value could be achieved with better estimation of the contact area for indentation. In this study the contact area was assumed to be the flat area of the indenter tip (0.0025mm^2), due to the small indentation depth (0.02mm). It is possible that in reality the contact area for the indentation is larger than that assumed in this study, due to the indenter tip geometry (Fig. 2). Future experiments will be conducted to determine a more accurate value for the contact area of the probe during indentation using inverse finite element, imaging, and mathematical methods. Although it is also possible that a different contact model would yield different results for the material properties, the primary goal of this research was to develop a micro-indentation device capable of measuring the mechanical properties of brain tissue at dynamic strain rates and present useful data on the characterization of brain tissue.

5. Conclusion

A custom-built micro-indentation device was developed that is capable of performing material characterisation tests at dynamic strain rates, up to 30/s with the current configuration, to determine how brain tissue from different regions respond to injurious loading scenarios. The apparatus is capable of measuring forces up to $10,000\mu\text{N}$ with a sampling rate of 10,000 samples per second and a maximum achievable velocity of 1000mm/s.

The material properties of two brain regions, the cortex and cerebellum, were characterized

using the device and an analytical solution. The murine cortex tissue (7.05 ± 3.92 kPa) was found to be significantly stiffer than the cerebellum tissue (3.59 ± 1.27 kPa). There was no statistically significant difference between the left and right hemispheres of the respective indentation regions, nor the anterior and posterior regions of the cortex. This appears to be the first report of micro-indentation tests being conducted at 30/s strain-rate for brain tissue. Future studies will focus on characterizing brain tissue at other dynamic strain rates and indentation depths to determine viscoelastic material properties.

A current limitation of the device is that the probe is sensitive to vibrations that are caused by the stepper motor and the linear stage movement. However, once the data has been post-processed in MATLAB, the force-displacement curve is smoothed and the effects of vibrations are removed. Future work will focus on removing these vibrations and automating the system to optimize the experimental procedure.

Acknowledgements

This work was supported by Science Foundation Ireland (Grant No. 12/IP/1732).

References

- Bernick K.B., Prevost T.P., Suresh S., Socrate S., 2011, Biomechanics of single cortical neurons, *Acta Biomaterialia*, 7, 1210-1219.
- Cheng S., Bilston L.E., 2007, Unconfined compression of white matter, *J. Biomech.*, 40, 117,124.
- El Sayed T., Mota A., Fraternali F., Ortiz M., 2008, Biomechanics of traumatic brain injury, *Comput. Methods Appl. Mech. Engrg.*, 197, 4692-4701.
- Elkin B.S., Ilankova A., Morrison III B., 2011, Dynamic regional mechanical properties of the porcine brain: Indentation in the coronal plane, *J. Biomech. Eng.*, 133, 071009-1-7.
- Faul M, Xu L, Wald MM, Coronado VG., 2010, Traumatic brain injury in the United States: emergency department visits, hospitalizations, and deaths. Atlanta (GA): Centers for Disease Control and Prevention, National Center for Injury Prevention and Control.
- Fountoulakis M., Hardmeier R., Hoyer H., Lubec G., 2001, Postmortem changes in the level of brain proteins, *Exp. Neurol.*, 167: 86-94.
- Gaetz M., 2004, The neurophysiology of brain injury, *Clinical Neurophysiology*, 115, 4-18.
- Gefen A., Margulies S. S., 2004, Are in vivo and in situ brain tissues mechanically similar?, *J. Biomech.*, 37, 1339-1352.
- Giordano C., Cloots R.J.H., van Dommelen J.A.W., Kleiven S., 2014, The influence of anisotropy on brain injury prediction, *J. Biomech*, 47, 1052-1059.
- Haslach Jr. H.W., Leahy L.N., Riley P. et al., 2014, Solid-extracellular fluid interaction and damage in the mechanical response of rat brain tissue under confined compression, *J. Mech. Behav. Biomed. Mat.*, 29, 138-150.
- Hendelman Walter J., *Atlas of Functional Neuroanatomy*, CRC Press, 2006, p66.

- Horgan T.J, Gilchrist M.D, 2003, The creation of three-dimensional finite element models for simulating head impact biomechanics, *Int. J. Crashworthiness*, 8(4), 353-366.
- Isidre F., Gabriel S., Arzberger T., et al., Brain protein preservation largely depends on the postmortem storage temperature: Implications for study of proteins in human neurologic diseases and management of brain banks: A BrainNet Europe study., *J. Neuropathol. & Exp. Neurol.*, 66(1): 35-46, 2007.
- Jin X., Zhu F., Mao H., Shen M., Yang K. H., 2013, A comprehensive experimental study on material properties of human brain tissue, *J. Biomech.*, 46, 2795-2801.
- Johnson K.L., 1985, *Contact Mechanics*, Cambridge University Press, Cambridge.
- Kleiven S., von Holst H., 2002, Consequences of head size following trauma to the human head, *J. Biomech.*, 35, 153-160.
- Lin D.C., Shreiber D.I., Dimitriadis E.K., Horkay F., 2009, Spherical indentation of soft matter beyond the Hertzian regime: numerical and experimental validation of hyperelastic models, *Biomech. Model Mechanobiol.*, 8, 345-358.
- Lu Y., Franze K., Seifert G., et al., 2006, Viscoelastic properties of individual glial cells and neurons in the CNS, *PNAS*, 103, 17759-17764.
- Maas SA, Ellis BJ, Ateshian GA, Weiss JA: FEBio: Finite Elements for Biomechanics. *Journal of Biomechanical Engineering*, 134(1):011005, 2012.
- Mao H, Zhang L, Jiang B, et al., 2013, Development of a finite element human head model partially validated with thirty five experimental cases, *J. Biomech. Eng.*, 135, 111002-111002-15.
- Mustata M., Ritchie K., McNally H.A., 2010, Neuronal elasticity as measured by atomic force microscopy, *J. Neurosci. Methods*, 186, 35-41.
- Ogden, R. W., 1972, Large Deformation Isotropic Elasticity - On the Correlation of Theory and Experiment for Incompressible Rubberlike Solids, *Proceedings of the Royal Society of London. Series A, Mathematical and Physical Sciences*, Vol. 326, No. 1567, pp. 565-584.
- Pervin F, Chen W.W, 2009, Dynamic mechanical response of bovine gray matter and white matter brain tissues under compression, *J. Biomech.*, 42, 731-735.
- Pharr G. M., Oliver W.C., Brotzen F.R., 1992, On the generality of the relationship among contact stiffness, contact area, and elastic modulus during indentation, *J. Mater. Res.*, 7, 613-617.
- Prange M.T, Margulies S.S, 2002, Regional, directional, and age-dependent properties of the brain undergoing large deformation, *J. Biomech. Eng.*, 124, 244-252.
- Prevost T. P., Balakrishnan A., Suresh S., Socrate S., 2011, Biomechanics of brain tissue, *Acta Biomaterialia*, 7: 83-95.
- Rashid B, Destrade M, Gilchrist M. D, 2012, Mechanical Characterization of brain tissue in simple compression at dynamic strain rates, *J. Mech. Behav. Biomed. Mat.*, 10, 23-38.
- Rashid B, Destrade M, Gilchrist M. D, 2013, Mechanical Characterization of brain tissue in simple shear at dynamic strain rates, *J. Mech. Behav. Biomed. Mat.*, 28, 71-85.
- Sanborn B., Nie X., Chen W., Weerasooriya T., 2012, Inertia effects on characterization of the dynamic response of brain tissue, *J. Biomech.*, 45, 434-439.

Figure Captions

Figure 1. Schematic Diagram of the Complete Test Apparatus

Figure 2. FemtoTools FTS-10000 Microforce Sensing Probe Dimensions

Figure 3. Regions and Indentation Sites of the Murine Brain. ● = Indentation Site

Figure 4. Experimental and Numerical Force Displacement Curves

Figure 1
[Click here to download high resolution image](#)

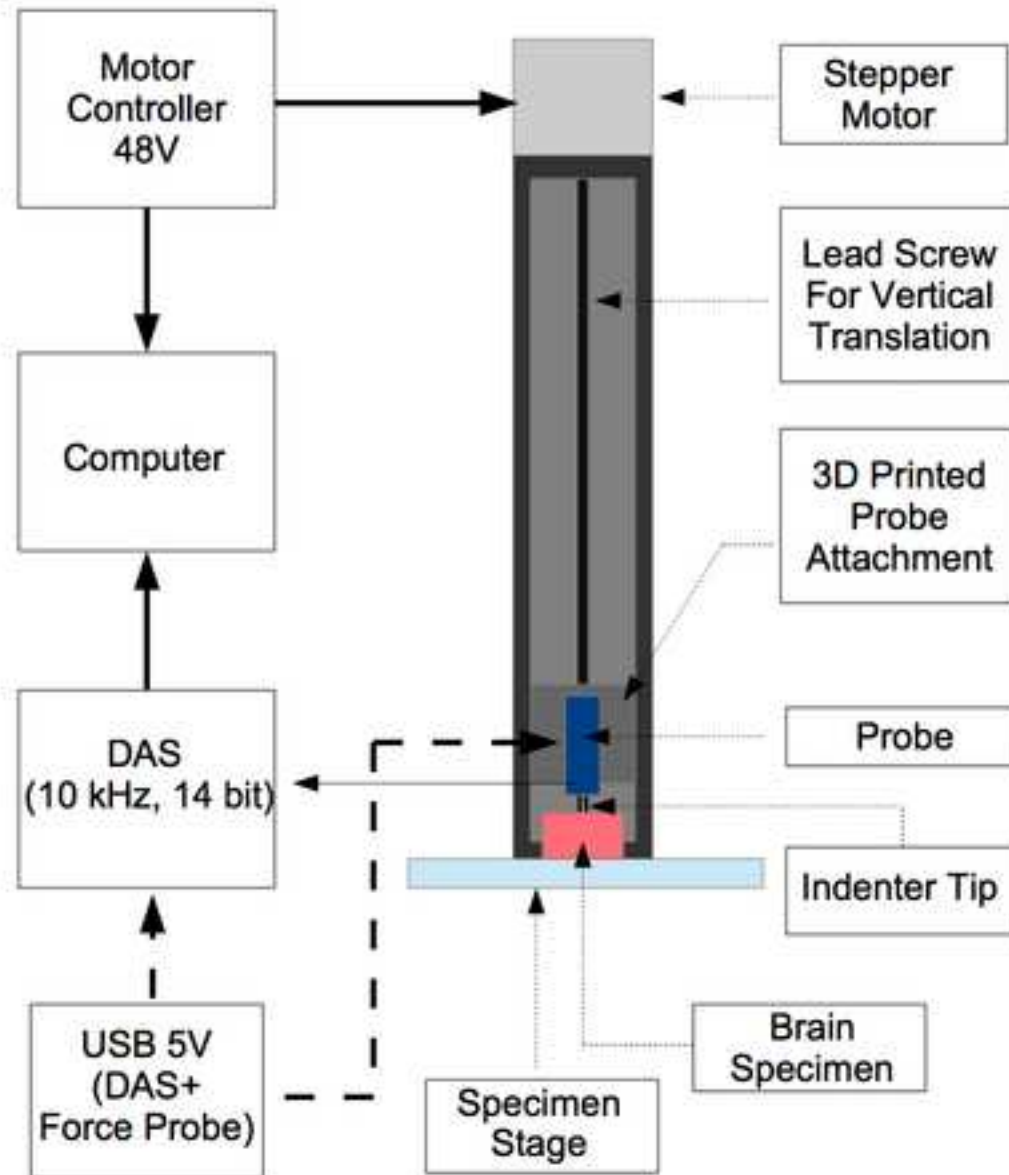


Figure 2
[Click here to download high resolution image](#)

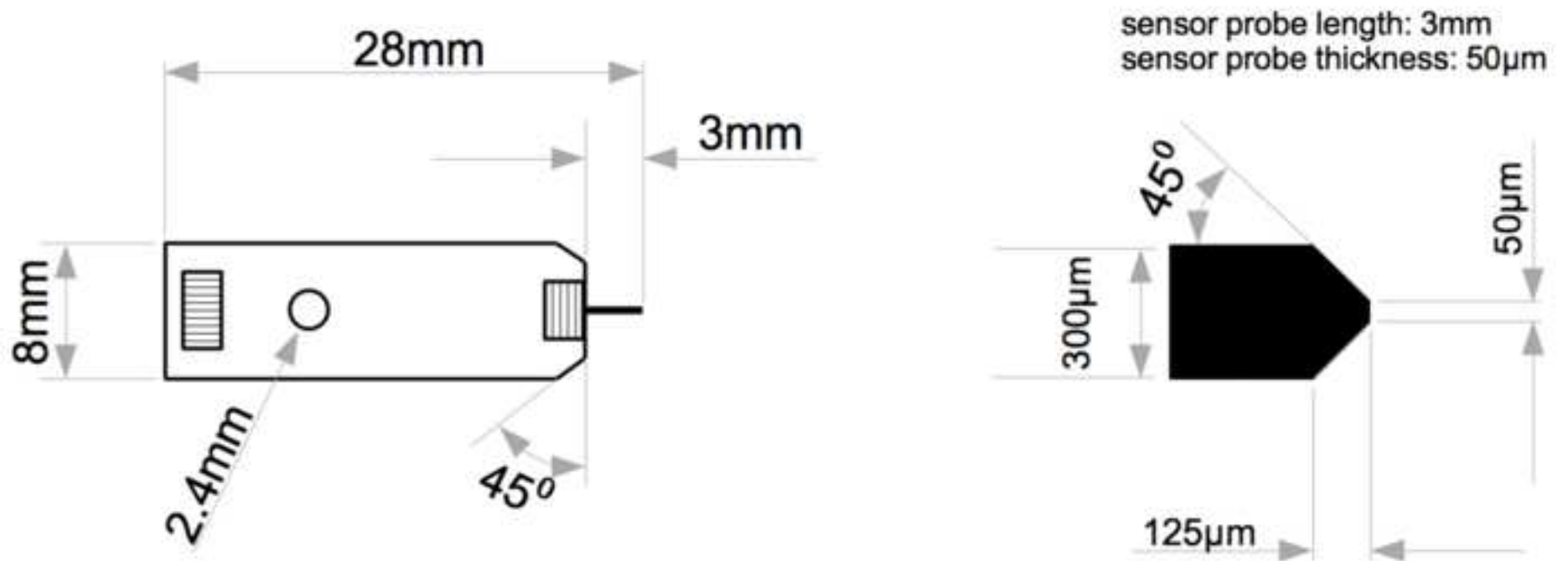


Figure 3
[Click here to download high resolution image](#)

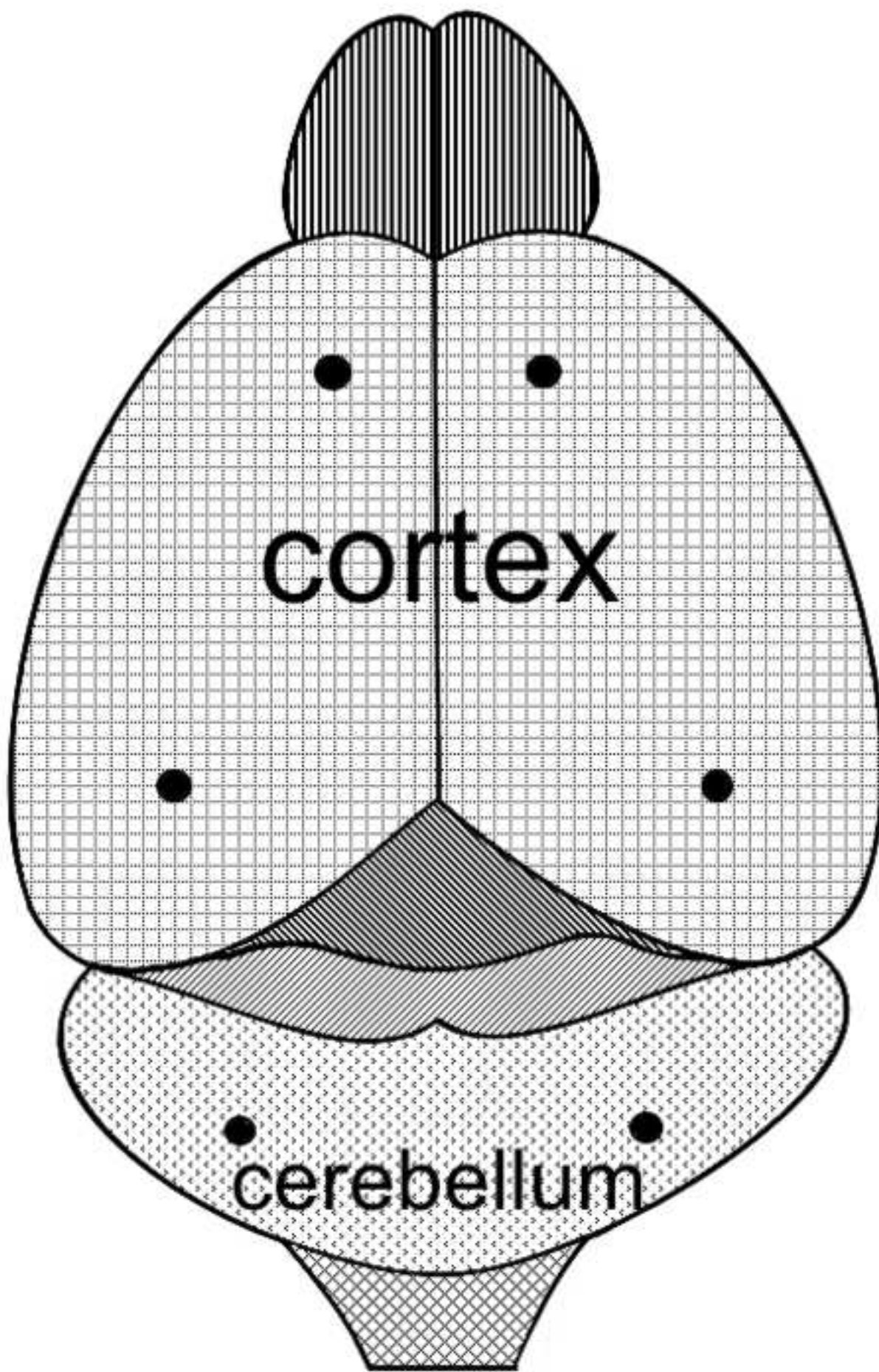


Figure 4

[Click here to download high resolution image](#)

